

Highly Selective Iron-Catalyzed Synthesis of Alkenes by the Reduction of Alkynes

Stephan Enthaler,^{*[a]} Michael Haberberger,^[a] and Elisabeth Irran^[b]

Abstract: Herein, the iron-catalyzed reduction of a variety of alkynes with silanes as a reductant has been examined. With a straightforward catalyst system composed of diiron nonacarbonyl and tributyl phosphane, excellent yields and chemo-selectivities (>99 %) were obtained for the formation of the corresponding alkenes. After studying the reaction conditions, and the scope and limitations of the reaction, several attempts were undertaken to shed light on the reaction mechanism.

Introduction

Alkenes have an extensive range of applications including, as synthons for bulk chemicals, pharmaceuticals, agrochemicals, polymers, in the syntheses of natural compounds, and as key intermediates in organic syntheses. During the last few decades, a number of methodologies have been established to access alkenes; of these, the reduction of alkynes is of great significance, because of the availability and low cost of the starting materials (alkynes, hydrogen, and hydrogen sources).^[1] Catalytic hydrogenation is the most-direct route to alkenes. In this regard, the application of transition metal complexes has been demonstrated as useful reduction catalysts to control the reaction.^[2] To date, several catalysts rely on precious metals, such as rhodium, ruthenium, iridium, or palladium. Owing to the high price and sometimes toxicity, less-expensive “biological” metal-based catalysts are highly desirable.^[3] Thus the use of iron is probably of great significance. During the last few years, the potential use of iron in synthetic transformations has been exhibited in various re-

duction processes, such as C=O, C=C, C=N, and NO₂ reductions.^[3,4] Indeed, iron catalysts have been applied for the reduction of alkynes to access alkenes using hydrogen as reductant.^[5] However, problems can arise by over-reduction to the corresponding alkane derivatives which reduce the impact of the method. Apart from over-reduction the (E)/(Z)-selectivity must be addressed by the catalysts. Here the routes to (Z)-alkenes are of interest.^[6] On the other hand, catalytic hydrosilylation is an alternative to hydrogenation, because of mild reaction conditions and simplicity. Furthermore, the silane functionality in the obtained products (alkenylsilanes) can be the starting point for additional transformations.^[7] Promising efforts were reported by the group of Chirik, who applied well-defined iron-complexes modified by tridentate nitrogen ligands to reduce alkynes with silanes to the corresponding alkene at ambient temperature.^[8] Even if an excellent iron-based procedure is available, the development of a general method to produce alkenes in an efficient and selective manner is still a desirable objective. Recently, we reported the reduction of sulfoxides in the presence of alkynyl groups to yield their corresponding sulfides, with significant amounts of alkene side-products.^[9,10] Based on these results, we wish to portray the application of a robust and easy-to-adopt iron-based catalyst for the highly selective reduction of alkynes to alkenes.

Results and Discussion

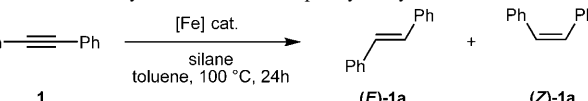
Initial studies on the influence of the reaction conditions were carried out with diphenylacetylene **1** as the model substrate by using 5.0 mol % of diiron nonacarbonyl and various

[a] Dr. S. Enthaler, M. Haberberger
Technische Universität Berlin
Department of Chemistry
Cluster of Excellence “Unifying Concepts in Catalysis”
Straße des 17. Juni 115
10623 Berlin (Germany)
Fax: (+49)3031429732
E-mail: stephan.enthaler@tu-berlin.de

[b] Dr. E. Irran
Institute of Chemistry: Metalorganics and Inorganic Materials
Technische Universität Berlin
Straße des 17. Juni 135, Sekr. C2, 10623 Berlin (Germany)

silanes as reducing reagent in toluene at 100 °C (Table 1, entries 1–4). Afterwards, the reaction was quenched under aqueous conditions. Best performance for the formation of stilbene was found for $(\text{EtO})_3\text{SiH}$ with yields of up to 80 %

Table 1. Iron-catalyzed reduction of diphenylacetylene **1**.

Entry ^[a]	Iron source [mol %]	Silane	Conv. [%]	Yield of stil- bene [%] ^[b]	(Z) -Selec- tivity [%]	
						1
				(E)-1a	(Z)-1a	
1	$\text{Fe}_2(\text{CO})_9$	PhSiH_3	60	>99	33	
2	$\text{Fe}_2(\text{CO})_9$	PMHS	59	>99	55	
3	$\text{Fe}_2(\text{CO})_9$	$(\text{EtO})_3\text{SiH}$	79	>99	84	
4	$\text{Fe}_2(\text{CO})_9$	Me_2PhSiH	72	>99	58	
5	$\text{Fe}(\text{CO})_5$	PMHS	22	>99	58	
6	$\text{Fe}_3(\text{CO})_{12}$	PMHS	31	>99	68	
7	$\text{FeCl}_2 \cdot 4\text{H}_2\text{O}$	PMHS	<1	—	—	
8	FeCl_3	PMHS	<1	—	—	
9	$\text{Fe}(\text{ClO}_4)_3$	PMHS	46	72	52	
10	$[\text{Fe}(\text{acac})_3]$	PMHS	47	>99	52	
11 ^[c]	$\text{Fe}_2(\text{CO})_9$	$(\text{EtO})_3\text{SiH}$	76	>99	84	
12 ^[d]	$\text{Fe}_2(\text{CO})_9$	$(\text{EtO})_3\text{SiH}$	82	>99	62	
13 ^[e]	$\text{Fe}_2(\text{CO})_9$	$(\text{EtO})_3\text{SiH}$	57	>99	86	
14 ^[f]	$\text{Fe}_2(\text{CO})_9$	$(\text{EtO})_3\text{SiH}$	<1	—	—	
15	—	$(\text{EtO})_3\text{SiH}$	<1	—	—	

[a] Reactions were carried out with 0.036 mmol iron precursor (5 mol %), 0.72 mmol diphenylacetylene, 0.79 mmol silane (1.1 equiv), 2.0 mL toluene, 24 h at 100 °C. The yield was determined by GC analysis (30 m Rxn-5 ms column, 40–300 °C, (Z)-stilbene: 8.02 min, (E)-stilbene: 9.12 min, **1**: 8.83 min) with dodecane (7.84 min) as internal standard. In the case of PMHS, 0.5 mL were used. [b] Combined yield of (E)- and (Z)-stilbene.

[c] THF, 60 °C. [d] Toluene, 60 °C. [e] THF, RT. [f] MeOH, 60 °C.

after 24 hours, with a (Z)-selectivity of 84 %. Other silanes, such as PhSiH_3 , Me_2PhSiH , and PMHS [poly(methylhydrosiloxane)] gave similar yields, but with lower *cis*-selectivity. Remarkably, the iron-catalyzed reduction of alkynes was highly selective, as no over-reduction to the corresponding 1,2-diphenylethane was observed. Moreover, different iron salts were tested (Table 1, entries 5–10), whilst in the absence of any iron salts no product was detected (Table 1, entry 15). However, no progress was achieved with respect to yield and (Z)-selectivity. Decreasing the reaction temperature to 60 °C did not improve the reaction outcome

Abstract in German: Im Rahmen dieser Arbeit wird die Eisen-katalysierte Reduktion von Alkinen zu den entsprechenden Alkenen mit Hilfe von Silanen vorgestellt. Hierbei konnten exzellente Ausbeuten und Selektivitäten (> 99 %) durch die Modifikation des eingesetzten Eisenkatalysators mit Phosphanen beobachtet werden. Nach genauer Untersuchung verschiedenster Reaktionsparameter wurden die hervorragenden Eigenschaften des Katalysatorsystems in der Reduktion zahlreicher Alkine gezeigt. Zum besseren Verständnis der Reaktion wurden verschiedene mechanistische Experimente durchgeführt.

(Table 1, entry 12). Using tetrahydrofuran as solvent under identical conditions resulted in 76 % yield and 84 % (Z)-selectivity. Importantly, the catalyst demonstrated comparable activity even when decreasing the temperature to 25 °C, with 57 % of (E)/(Z)-stilbene detected after one day (Table 1, entry 13). Besides, the reduction of the catalyst loading to 1 mol % resulted in a diminished yield.

To improve the catalyst performance, the influence of various nitrogen-containing ligands were studied (Table 2, entries 2–8). The highest (Z)-selectivity was detected for phenanthroline **5** (92 %) and 2,2'-bipyridine **4** (86 %), but with lower conversions. In addition, monodentate and bidentate phosphane ligands were applied in combination with $\text{Fe}_2(\text{CO})_9$ (Table 2, entries 9–14). Excellent (Z)-selectivity was observed for simple tributyl phosphane (96 %) and (1,1'-bis(diphenylphosphino)ferrocene) (dppf; 92 %). Furthermore, performing the reaction at room temperature improved the *cis*-selectivity for the $\text{Fe}_2(\text{CO})_9$ /tributyl phosphane system to >99 % (Table 2, entry 9). To identify the role of the phosphane in the reaction, the phosphorus–selenium coupling constants [$J(^3\text{P}-^7\text{Se})$] were compared to estimate the σ -donor ability of the phosphanes. It has been reported that the magnitude of the coupling constant can be correlated to basicity, with an increase in the basicity of the phosphanes leading to higher coupling constants.^[11] However, in the monodentate series, PBu_3 ($J=680$ Hz), $\text{P}-(2,6-(\text{MeO})_2\text{Ph})_3$ ($J=717$ Hz), BuPAd_2 ($J=680$ Hz), as well as in the bidentate series dppf ($J=737$ Hz) and dppe ($J=736$ Hz), no correlation with the reaction outcome was observed.^[12]

Moreover, the time-dependency of the (Z)-selectivity of stilbene **1a** was studied. Samples were taken over time, according to the experiment stated in Table 2 entry 9 (60 °C). No significant differences in (Z)-selectivity were observed (>90 % in all cases).

To explore the scope and limitation of this iron catalyst ($\text{Fe}_2(\text{CO})_9/\text{PBu}_3$), a variety of alkyne substrates were tested under the reaction conditions given in Table 2 entry 9 (60 °C). First, various substituted diphenyl acetylenes were reacted with $(\text{EtO})_3\text{SiH}$ (Table 3). In all cases, the reaction time was prolonged to 48 hours to ensure higher conversion. No significant effect was observed in the presence of electron-withdrawing or electron-donating groups (Table 3, entries 1–9). However, a decrease of the (Z)-selectivity was noticed compared to the reduction of parent compound **1**, but the chemoselectivity for alkene formation was still excellent (>99 %). Difficulties were observed for compound **22** which contained a nitro group at the *para*-position (Table 3, entry 9); here, some reduction of the nitro group to the corresponding amine was found. Importantly, the reduction of the nitro group decreases the reactivity of the alkenyl moiety because only the (4-aminophenyl)-phenylacetylene was detected, whilst the corresponding 4-amino stilbene was not observed. Good performance was demonstrated for the reduction of alkynes containing heteroaromatic groups (Table 3, entry 10). Interestingly, the (E)-isomer was formed as the major compound. Moreover, phenyl acetylene as the

Table 2. Iron-catalyzed reduction of diphenylacetylene **1** in the presence of N- or P-ligands.

Entry	Ligand	M/L ^[b]	Conv. [%]	Yield of Stilbene [%] ^[b]	(Z)-Selectivity [%]	5 mol% Fe ₂ (CO) ₉ ligand	Diphenylacetylene 1	(E)- 1a	(Z)- 1a
						(EtO) ₃ SiH	THF, 60 °C, 24 h		
1	–	–	–	>99	84				
2	Me ₂ N-CH ₂ -NMe ₂	2	1:1	>99	48				
3	Me ₂ N-CH ₂ -CH ₂ -NMe ₂	3	1:1	42	>99				
4		4	1:1	52	>99				
5		5	1:1	63	>99				
6		6	1:2	<1	–				
7 ^[11]		7	1:2	77	>99				
8	Mes-N=C=N-Mes	8	1:1	79	>99				
9 ^[c]	PBu ₃	9	1:2	68 (64)	>99 (>99)				
10	P(2,6-(MeO) ₂ Ph) ₃	10	1:2	73	>99				
11	BuPAd ₂	11	1:2	87	>99				
12 ^[c]		12	1:1	79 (59)	>99 (>99)				
13		13	1:1	85	>99				
14		14	1:1	45	>99				

[a] Reactions were carried out with 0.036 mmol Fe₂(CO)₉ (5 mol%), 0.036 mmol or 0.0072 mmol ligand (5–10 mol%), 0.72 mmol diphenylacetylene, 0.79 mmol (EtO)₃SiH (1.1 equiv), 2.0 mL THF, 24 h at 60 °C. The yield was determined by GC analysis (30 m Rx-5 ms column, 40–300 °C, (Z)-stilbene: 8.02 min, (E)-stilbene: 9.12 min, **1**: 8.83 min) with dodecane (7.84 min) as an internal standard. [b] Combined yield of (E)- and (Z)-stilbene. [c] In parenthesis: 48 h at RT.

substrate yielded styrene in excellent yields (>99%) with an alkene-selectivity of 95%, whilst the double reduced product (ethyl benzene) was formed as a side-product (Table 3, entry 12). The reduction of the conjugated system **26** showed as main transformation the reduction of one triple bond (75%), whilst the reduction of both alkenyl groups were observed with 15% (Table 3, entry 13). In addition, substrates containing functional groups attached to the triple bond were subjected to catalysis (Table 3, entries 15–18). In the case of ester functionalities, a mixture of the corresponding esters of fumaric acid and maleic acid were obtained in excellent yields. Worthy of note is that the reduction was highly selective to alkenyl reduction, whilst the ester groups were not reduced under the described conditions.

In order to study the selectivity of the process, different substrates containing functional groups sensitive to reduction or a combination of the diphenylacetylene with an additional substrate were reacted with triethoxysilane in the

presence of Fe₂(CO)₉ (Table 4). Excellent chemoselectivity (>99%) was observed for the reduction of alkynes in the presence of aldehydes, esters, amides, C=C double bonds, and epoxides, whilst ketones (43%) and sulfoxide groups (7%) were reduced to some extent.

Afterwards, competitive-reduction experiments of *m/p*-substituted substrates were carried out. Equimolar amounts of diphenylacetylene (0.72 mmol) and substituted diphenylacetylene (0.72 mmol) were reacted with triethoxysilane (0.72 mmol) in the presence of the in situ generated catalyst (Fe₂(CO)₉/PBu₃).

The reaction mixture was hydrolyzed after 24 hours and the yields of both compounds and their corresponding isomers was determined by GC analysis and correlated with the Hammett σ^+ (Figure 1).^[13] The values were correlated after $\log(k_X/k_H) = \rho\sigma^+$. However, no helpful information was obtained for the single isomers. A value of $R^2 = 0.82$ was achieved for the summation of the isomers. Linear regression analysis led to a reaction constant value of 0.99 for both isomers.

The positive Hammett value indicated a partial negative charge in the transition state in comparison with the starting substrates.

To gain additional insight into the reaction mechanism, the carbon–carbon triple bond was applied as a probe. First, the ¹³C NMR data can be of interest for studying the effect of diphenyl-acetylene substitution and the electronic features of the triple bond on the reaction outcome. DFT calculations at the RB3LYP/6-31(d) level were carried out to model the magnetic properties using the Gauge Independent Atomic Orbital (GIAO) technique.^[14,15] The accuracy of this method compared to experimental values has been reported by Gevorgyan and co-workers.^[16] The GIAO shielding was related to the obtained yields for both product isomers (Figure 2 and Figure 3). Importantly, both triple-bonded carbon atoms are non-equivalent owing to different substitution patterns. As seen in Figure 2 and Figure 3, no strong correlation between the GIAO shielding and the catalytic results was found.

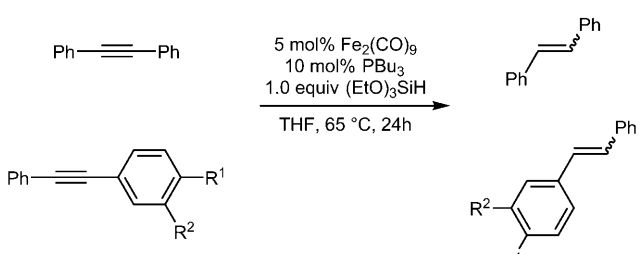
Table 3. Scope and limitations of the iron-catalyzed reduction of alkynes.

Entry ^[a]	Substrate	Conv. [%] ^[b]	<i>cis/trans</i> ^[c]	
			(E)-1a, 15a–31a	(Z)-1a, 15a–31a
1	Ph—C≡C—Ph	1	68 (>99) ^[d]	>99:<1
2	Ph—C≡C—(p-Me)Ph	15	58 (>99)	88:12
3	Ph—C≡C—(m-Me)Ph	16	72 (>99)	75:25
4	Ph—C≡C—(p-iBu)Ph	17	57 (>99)	80:20
5	Ph—C≡C—(p-OMe)Ph	18	62 (>99)	61:39
6	Ph—C≡C—(m-OMe)Ph	19	53 (>99)	79:21
7	Ph—C≡C—(p-F)Ph	20	48 (>99)	78:22
8	Ph—C≡C—(m-F)Ph	21	63 (>99)	78:22
9	Ph—C≡C—(p-NO ₂)Ph	22	89 (66) ^[e]	63:37
10	Ph—C≡C—(p-pyridyl)Ph	23	55 (>99)	36:64
11	Ph—C≡C—(p-CH ₂ CH ₂ CH ₃)Ph	24	44 (>99)	99:1
12	Ph—C≡C—Ph	25	>99 (95) ^[f]	--
13	Ph—C≡C—Ph	26	75 (60) ^[g]	63:37
14	Ph—S—C≡C—Ph	27	85 (76) ^[h]	--
15	Ph—C≡C—COOEt	28	83 (>99)	19:81
16	MeOOC—C≡C—COOMe	29	>99 (>99)	43:57
17	EtOOC—C≡C—COOEt	30	80 (>99)	15:85
18	Me ₃ Si—C≡C—SiMe ₃	31	>99 (>99)	83:17

[a] Reactions were carried out with 0.036 mmol Fe₂(CO)₉ (5 mol %), 0.072 mmol PBu₃, 0.72 mmol substrate, 0.79 mmol (EtO)₃SiH (1.1 equiv), 2.0 mL THF, 48 h at 60°C. The conversion was determined by GC (30 m Rxi-5 ms column, 40–300°C) and ¹H NMR analysis. [b] Chemoselectivity for alkene formation is given in parenthesis. [c] Determined by GC (30 m Rxi-5 ms column, 40–300°C) and ¹H NMR analysis. [d] 24 h. [e] 4-H₂N-PhCCPh was observed as a side-product. [f] Phenylethane (5%) was observed as a side-product. [g] The reduction of both triple bonds was observed (15%) as a side-reaction. [h] Thiophenol was observed as a side product (9%).

Secondly, the value for the stretch of the carbon–carbon triple bond was correlated to the results. Owing to the weakness of the stretch, the values were calculated using DFT at the RB3LYP/6-31(d) level. Similar to the GIAO shielding, no precious information were attained (Figure 4). Based on the Hammett-plot and the calculations, the reaction is probably comprised of various reaction pathways, which lead to an undefined picture.

Moreover, several iron complexes were synthesized by reacting equimolar amounts of monodentate phosphane **10** or bidentate dppf **13** with diiron nonacarbonyl in refluxing diethylether. In both cases, single-crystals suitable for X-ray diffraction analysis were obtained by cooling the solution to



15: R¹ = Me, R² = H **18:** R¹ = H, R² = OMe
16: R¹ = tBu, R² = H **19:** R¹ = F, R² = H
17: R¹ = MeO, R² = H

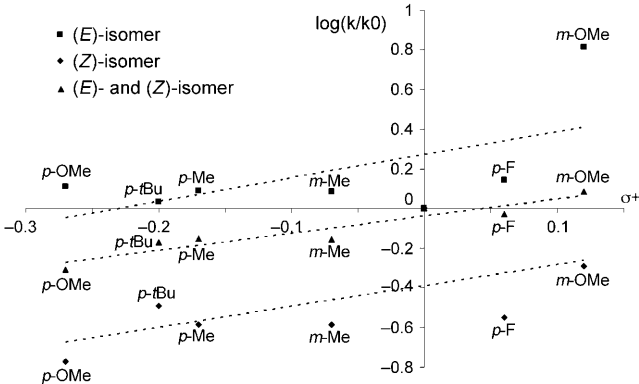


Figure 1. Hammett correlation for the reduction of *p/m*-substituted diphenylacetylene [$\log(k/\text{substituted})/k\theta/\text{unsubstituted}) = \rho\sigma^+$; $\rho = 0.9857$; R² = 0.82 for summation of both isomers].

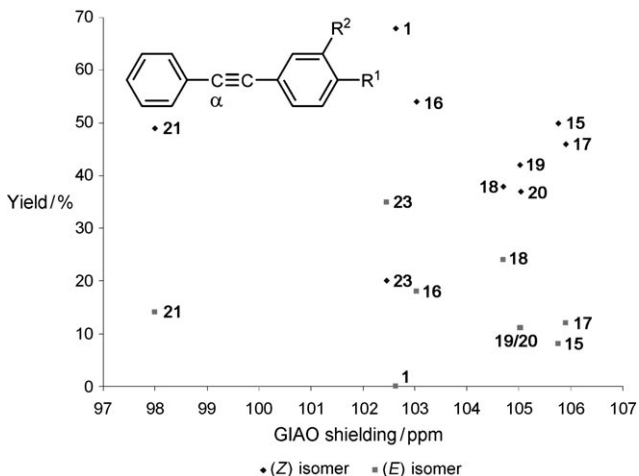


Figure 2. Correlation of the yield and the GIAO shielding of the alkenyl α -carbon.

room temperature and slow evaporation of the solvent. Thermal ellipsoid plots for the complexes are displayed in Figure 5 and Figure 6. In case of the mononuclear complex **41**, one monodentate phosphane is coordinated to the iron center, whilst in case of the bidentate phosphane, both phosphorous donors are attached to the metal. Those coordination motifs have been reported recently.^[17] In complex **41**, four carbonyl ligands are coordinated to the iron center. For the *trans*-positioned carbonyl ligand, with respect to the

Table 4. Functional group tolerance of the iron-catalyzed reduction of alkynes.

Entry	Substrate	Additive	Yield of Alkyne Reduction [%] ^[b]	Yield of Second Additive [%]
				(E)-1a
1	Ph—C≡C—Ph	32	55 (>99)	>99 ^[c]
2	Ph—C≡C—Ph	33	61 (>99)	43
3	Ph—C≡C—Ph	34	83 (>99)	<1
4	Ph—C≡C—Ph	35	67 (>99)	<1
5	Ph—C≡C—Ph	36	17 (>99)	<1
6	Ph—C≡C—Ph	37	98 (>99)	<1
7	Ph—C≡C—Ph	38	32 (>99)	7
8	Ph—C≡C—Ph	39	>99 (>99)	<1
9	Ph—C≡C—Ph	40	66 (57)	<1

[a] Reactions were carried out with 0.036 mmol $\text{Fe}_2(\text{CO})_9$ (5 mol %), 0.072 mmol PBu_3 , 0.72 mmol **1**, 0.72 mmol additional substrate, 0.79 mmol $(\text{EtO})_3\text{SiH}$ (1.1 equiv), 2.0 mL THF, 48 h at 60°C. The yield was determined by GC (30 m RxI-5 ms column, 40–300°C). [b] (Z)-selectivity is given in parentheses. [c] Undefined side-products.

phosphane ligand, a shorter Fe–C distance (2.920 Å) were observed as for the *cis*-carbonyl ligands (2.928–2.938 Å) because of the *trans*-effect of the Fe–P bond. In addition, the Fe–P bond length is 2.338 Å, which is slightly longer than

that determined for the bidentate system (2.242–2.254 Å).^[17] The triaryl moiety of the monodentate system is pyramidal arranged and slightly distorted owing to the influence of the $\text{Fe}(\text{CO})_4$ unit compared to similar complexes. The distortion angles of the three phenyl groups are 37°, 44°, and 65°. The P–C bond distances are nearly equal (1.842–1.848 Å).

In complex **42**, the cyclopentadienyl rings ($\text{C}_{\text{ipso}}\text{-P-P'-C'}_{\text{ipso}}$) are eclipsed by an angle of 29.5° and the distances of Fe–P bonds are nearly equal (2.242 and 2.254 Å). Owing to the bidentate coordination, only three positions on the metal are blocked by carbonyl ligands. Furthermore, the ligand spanned a bite angle of 99.9°, which is in accordance to the structure reported by Shim and co-workers.^[18]

The IR spectra of **41** shows three strong CO stretching bands at 1981, 1908, and 1880 cm^{-1} , whilst for **42**, two strong CO stretching bands at 2028 and 1912 cm^{-1} and two weak bands at 2186 and 2119 cm^{-1} were observed. In

the ^1H NMR spectra of complex **41**, a significant signal at 3.22 ppm was attributed to the methoxy-groups, whilst for **42**, the characteristic cyclopentadienyl signals were found.

The isolated complexes were then subjected to the catalytic reduction of diphenylacetylene **1** under the reaction

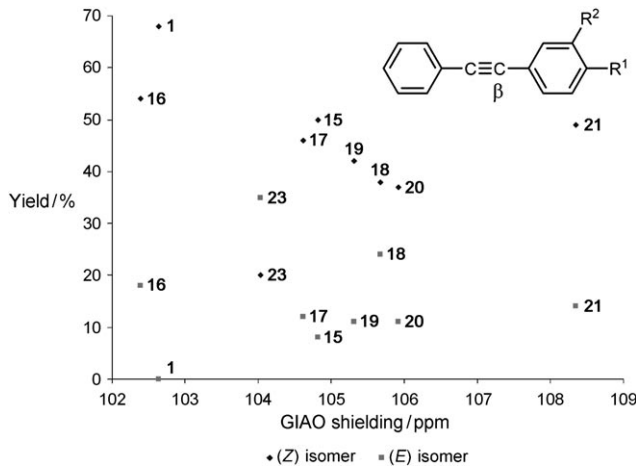


Figure 3. Correlation of the yield and the GIAO shielding of the alkenyl β -carbon.

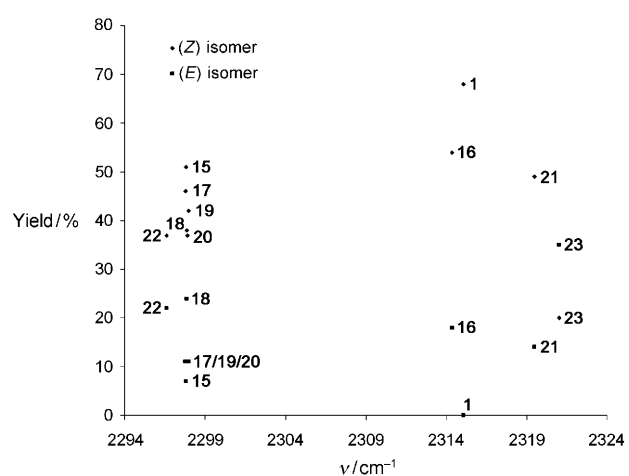


Figure 4. Correlation of the yield with triple bond stretch.

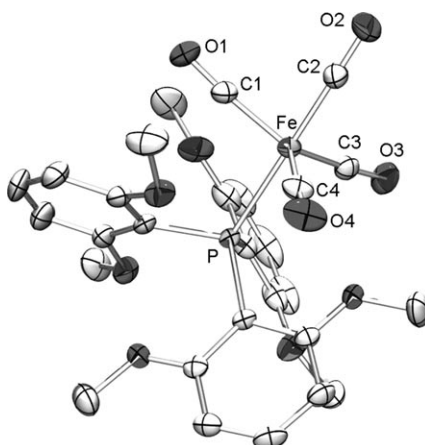


Figure 5. Molecular structure of $(\text{10})\text{Fe}(\text{CO})_4$ (**41**). Hydrogen atoms are omitted. Thermal ellipsoids are drawn at the 50% probability level. Selected bond distances [\AA]: Fe-C2: 1.762(2), Fe-C: 1.782(2)-1.793(3), Fe-P: 2.3387(6).

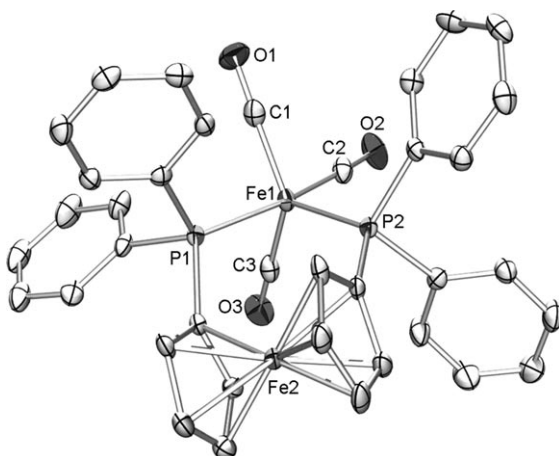
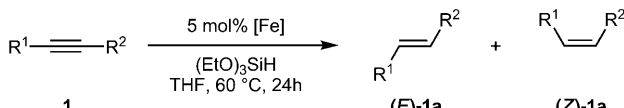


Figure 6. Molecular structure of $(\text{dppf})\text{Fe}(\text{CO})_3$ (**42**). Hydrogen atoms are omitted. Thermal ellipsoids are drawn at the 50% probability level. Selected bond distances [\AA] and angles [$^\circ$]: Fe1-C: 1.767(3)-1.782(3), Fe-P: 2.2421(8)-2.2541(8), P1-Fe1-P2: 99.87(3).

conditions described in Table 2 (Scheme 1). Comparing the results for the isolated- and well-defined complexes with the *in situ* concept, an improved performance was noticed for the *in situ* approach. In the case of complex **42**, Kim, Shim and co-workers reported the formation of various iron-containing side-products during the preparation of complex **42**.



41: yield: 42%, alkene selectivity >99%, (*Z*)-selectivity 88%
in situ: 73%, >99%, 88%
42: yield: 41%, alkene selectivity >99%, (*Z*)-selectivity 78%
in situ: 79%, >99%, 92%

Scheme 1. Comparison of isolated complexes with the *in situ* approach.

Those undefined iron complexes presumably also display catalytic activity. Unfortunately the side-products could not be fully characterized.

In addition, complexes **41** and **42** were reacted with either stoichiometric amounts of alkyne **1** or $(\text{EtO})_3\text{SiH}$ to try to isolate the intermediate species. However, various attempts, including heating, light irradiation, or the addition of Me_3NO to replace a carbonyl ligand by alkyne or silane ligands.

Although the precise mechanism is still unknown, different experiments were performed with the isolated complexes to hopefully shed some light on the mechanism. Initial mechanistic investigations were dedicated to the activation of the silane by complex **42**. The interaction of complex **42** with $(\text{EtO})_3\text{SiH}$ was studied in the absence of substrate by ^1H NMR spectroscopy. No signal was found for an iron-hydride species in the expected region. Based on this result, the formation of an iron-hydride species can be probably excluded on the NMR time-scale.^[8] Furthermore, owing to the paramagnetic abilities of the iron species, only broad signals were observed in NMR studies, which did not allow any valuable analysis. Moreover, the reaction was studied by solution IR methods, by applying the CO-ligands coordinated to the iron as a probe (Figure 7). First, $\text{Fe}_2(\text{CO})_9$ was dissolved

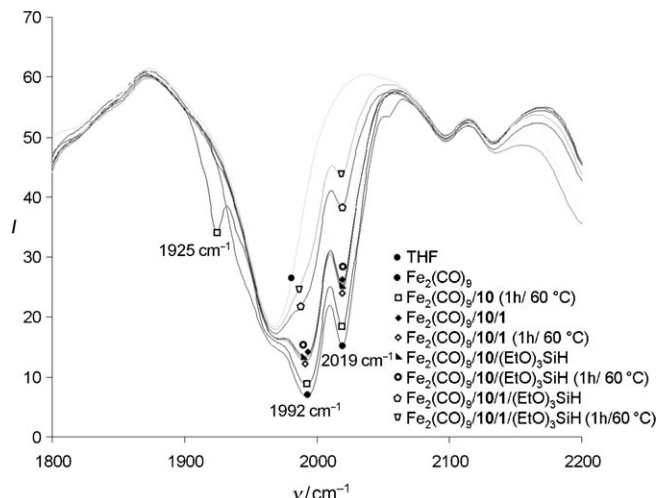
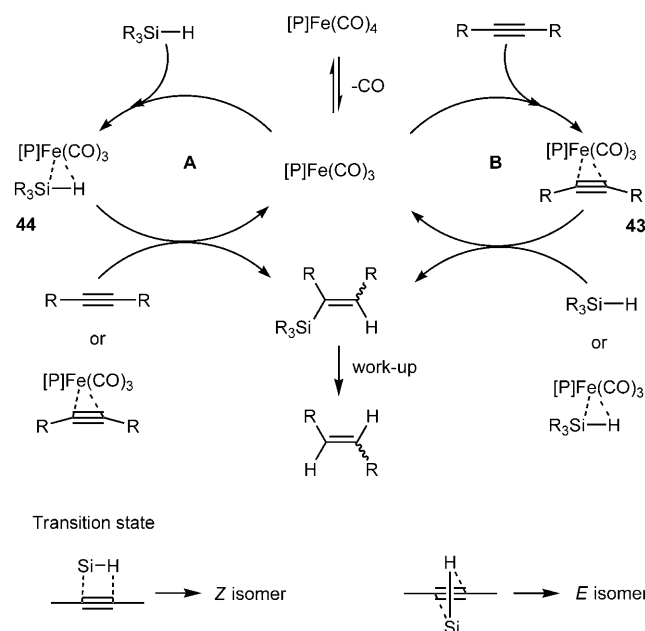


Figure 7. IR spectroscopic investigation into the interaction of $\text{Fe}_2(\text{CO})_9$, **10**, **1** and $(\text{EtO})_3\text{SiH}$ in THF.

in tetrahydrofuran and the appearance of two bands at 2019 and 1992 cm^{-1} , which can be ascribed to the mode of the carbonyl ligands. Next, ligand **10** was added and a spectrum was acquired after 1 hour at 60 °C; the spectrum showed, aside from the bands at 2019 and 1992 cm^{-1} , a band at 1925 cm^{-1} that was probably caused by coordination of the phosphine to the iron. The addition of either alkyne **1** (10 equiv) or $(\text{EtO})_3\text{SiH}$ (10 equiv) to this solution did not affect the bands at 2019 and 1992 cm^{-1} , while the band at 1925 cm^{-1} disappeared. Finally, all components ($\text{Fe}_2(\text{CO})_9/\text{10/1}/(\text{EtO})_3\text{SiH}$) were reacted in tetrahydrofuran resulted in the disappearance of the band at 1992 cm^{-1} and a significant

decrease in the band at 2019 cm^{-1} . The disappearance of one carbonyl band can be probably attributed to the dissociation of carbonyl ligands to allow new coordination sides for the alkyne or silane.

Based on our results, and previous reports we have proposed a catalytic mechanism illustrated in Scheme 2. In the initial step, one carbonyl ligand dissociates (see Figure 7)



Scheme 2. Potential reaction pathways for the reduction of alkynes with iron catalysts.

and forms an unsaturated iron species that either coordinates the alkyne or the silane (Scheme 2, cycle A and B). For both pathways, Chirik and co-workers were able to characterize the iron–alkyne and iron–silane complexes.^[8] Unfortunately, suitable intermediates could be isolated for neither the coordination of the silane nor the coordination of the alkyne. Activation of the C–C triple bond, owing to the coordination of the alkyne, allows interactions with the silane and finally the formation of the alkene (Scheme 2, cycle B). Furthermore, the reactions of both the iron–alkyne and iron–silane complexes can be seen as possible pathways to afford the hydrosilylated product. Same fact can be assumed for the iron–silane complex (Scheme 2, cycle A). Because no iron–hydride species was detected, we assume a concerted mechanism for the transfer of the Si–H functionality via a four-membered transition state (Scheme 2). Two possibilities can be envisaged: For the (*Z*)-addition, the activated alkyne and silane are horizontal to each other in the transition state, whilst for the (*E*)-addition, the alkyne and the silane are positioned orthogonal to one another (Scheme 2). As seen in Table 1 and Table 2, the (*Z*)/(*E*)-ratio is strongly depended on the addition of a ligand and the nature of the ligand; disfavoring of the (*E*)-addition was probably derived from the creation of a pocket and chang-

ing of the electronic structure of the metal. Furthermore, the (*E*)-isomer is favored in the case of functional groups closely connected to the triple bond, which could be addressed to a different coordination mode of the substrate to the metal centre.

Conclusions

In summary, we have demonstrated the value of iron as a catalyst in the reduction of alkynes to generate the corresponding alkenes. The simplicity of the procedure is outlined by the application of the commercially available metal source $\text{Fe}_2(\text{CO})_9$, modified by simple PBu_3 , and $(\text{EtO})_3\text{SiH}$ as a hydride source under mild and non-inert conditions. The outstanding selectivity of the system was shown by the reduction of several substrates with excellent yields and a broad functional-group tolerance.

Experimental Section

General

All manipulations with oxygen- and moisture-sensitive compounds were performed under a nitrogen atmosphere using standard Schlenk techniques. Toluene and tetrahydrofuran were distilled over sodium/benzophenone ketyl under a nitrogen atmosphere. ^1H and ^{13}C NMR spectra were recorded on a Bruker AFM 200 spectrometer (^1H : 200.13 MHz; ^{13}C : 50.32 MHz, ^{19}F : 188.33 MHz) using the proton signals of the deuterated solvents as reference. Single-crystal X-ray diffraction measurements were recorded on an Oxford Diffraction Xcalibur S Sapphire spectrometer. IR spectra were recorded either on a Nicolet Series II Magna-IR-System 750 FTR-IR or on a Perkin-Elmer Spectrum 100 FT-IR. Electron-impact mass spectra (EI-MS) were recorded on a Finnigan MAT95S. GC-MS measurements were carried out on a Shimadzu GC-2010 gas chromatograph (30 m Rx-5 ms column) linked with a Shimadzu GCMA-QP 2010 Plus mass spectrometer.

Safety Considerations

During our studies we used triethoxysilane as a reducing reagent without incident. However, Berk and Buchwald reported difficulties when working with triethoxysilane.^[21]

General Procedure for the Synthesis of Alkenes (Method A)

Reactions were carried out in accordance with the procedure reported by Liu and co-workers with small variations.^[19a] An aqueous solution of CuI (10 mol %, 0.8 mmol) and PPh_3 (20 mol %, 1.6 mmol) was stirred for 10 min at room temperature. This mixture was added to an aqueous solution of phenylacetylene (9.6 mmol), KOH (16.0 mmol), and the corresponding substituted iodoarene (8.0 mmol). The flask was sealed and heated to 120°C. After four days, the mixture was cooled to room temperature and the aqueous layer was extracted with diethyl ether (3×50 mL). The organic layer was washed with water, brine, and dried over Na_2SO_4 . The solvent was removed under vacuum and the residue was either purified by column chromatography on silica gel (*n*-hexane/ethyl acetate 98:2 to 4.5:1) or by crystallization.^[19]

(4-Methoxyphenyl)phenylacetylene (18)

Yield 92% (colorless crystals obtained by crystallization from diethyl ether); ^1H NMR (200 MHz, CDCl_3 , 25°C): $\delta = 7.30\text{--}7.64$ (7H, m, Ar), 6.90–6.98 (2H, m, Ar), 3.87 ppm (s, 3H, OCH_3); ^{13}C NMR (50.32 MHz, CDCl_3 , 25°C): $\delta = 159.6$, 133.0, 131.4, 128.3, 127.9, 123.6, 115.3, 114.0, 89.4, 88.0, 55.2 ppm; IR (KBr): $\tilde{\nu} = 3055$ (w), 2994 (w), 2958 (w), 2936 (w), 2835 (w), 2216 (w), 1604 (m), 1594 (m), 1510 (s), 1486 (m), 1465

(m), 1454 (m), 1440 (m), 1288 (m), 1246 (s), 1180 (m), 1139 (w), 1108 (m), 1070 (w), 833 (s), 813 (m), 779 (w), 755 (s), 692 (s), 523 cm⁻¹ (m); MS (70 eV, EI) *m/z* (%)=208 (100, *M*⁺), 193 (70), 165 (47), 139 (12), 104 (14).

(4-Fluorophenyl)phenylacetylene (**20**)

Yield 89% (colorless crystals obtained by crystallization from diethyl ether); ¹H NMR (200 MHz, CDCl₃, 25°C): δ =7.35–7.47 (m, 4H, Ar), 7.18–7.29 (m, 3H, Ar), 6.86–6.99 ppm (m, 2H, Ar); ¹³C NMR (50.32 MHz, CDCl₃, 25°C): δ =164.9, 160.0, 133.5, 133.3, 131.5, 128.32, 128.28, 123.1, 119.4, 119.3, 115.8, 115.4, 89.0, 88.3 ppm; IR (KBr): $\tilde{\nu}$ =3049 (w), 1594 (m), 1509 (s), 1217 (s), 1157 (m), 1098 (w), 911 (w), 843 (s), 815 (w), 792 (m), 755 (s), 688 (s), 516 (s), 493 cm⁻¹ (s); MS (70 eV, EI) *m/z* (%)=196 (100, *M*⁺), 175 (13), 170 (15), 98 (19), 85 (14).

(4-Methylphenyl)phenylacetylene (**15**)

Yield 77%; ¹H NMR (200 MHz, CDCl₃, 25°C): δ =7.38–7.66 (m, 7H, Ar), 7.20–7.28 (m, 2H, Ar), 2.45 ppm (s, 3H, CH₃); ¹³C NMR (50.32 MHz, CDCl₃, 25°C): δ =138.3, 131.51, 131.46, 129.1, 128.3, 128.0, 123.5, 120.2, 89.6, 88.7, 21.4 ppm; IR (KBr): $\tilde{\nu}$ =3049 (w), 2912 (w), 1594 (m), 1509 (s), 1440 (m), 1106 (w), 1070 (w), 916 (w), 818 (s), 754 (s), 690 (s), 515 cm⁻¹ (s); MS (70 eV, EI) *m/z* (%)=192 (100, *M*⁺), 165 (18), 95 (12); *R*_f=0.41 (*n*-hexane/ethyl acetate 4.5:1).

(4-Nitrophenyl)phenylacetylene (**22**)

Yield 81% (colorless crystals obtained by crystallization from diethyl ether); ¹H NMR (200 MHz, CDCl₃, 25°C): δ =8.06–8.15 (m, 2H, Ar), 7.60–7.51 (m, 2H, Ar), 7.40–7.50 (m, 2H, Ar), 7.24–7.33 (m, 3H, Ar), 7.13–7.18 ppm (m, 1H, Ar); ¹³C NMR (50.32 MHz, CDCl₃, 25°C): δ =146.8, 132.2, 131.8, 130.2, 129.2, 128.5, 123.6, 122.1, 94.7, 87.5 ppm; IR (KBr): $\tilde{\nu}$ =2925 (w), 2851 (w), 1592 (m), 1510 (s), 1345 (s), 1105 (m), 921 (w), 856 (m), 765 (m), 689 cm⁻¹ (m); MS (70 eV, EI) *m/z* (%)=223 (100, *M*⁺), 193 (30), 176 (62), 165 (20), 151 (25), 88 (15); *R*_f=0.49 (*n*-hexane/ethyl acetate 4.5:1).

General procedure for the synthesis of alkynes (Method B)

To a solution of phenyl acetylene (10.7 mmol) and the corresponding bromoarene (9.8 mmol) in dioxane (2.0 mL) was added palladium(II) chloride (5 mol %, 0.49 mmol), PPh₃ (10 mol %, 0.98 mmol), and triethyl amine (21.4 mmol). The mixture was stirred for 3 days at 60°C. Afterwards, the mixture was cooled to room temperature and dichloromethane (50 mL) was added. The organic layer was washed with water, brine, and dried over Na₂SO₄. The solvent was removed under vacuum and the residue was purified by column chromatography on silica gel (*n*-hexane/ethyl acetate 98:2 to 4.5:1).^[19]

(3-Methoxyphenyl)phenylacetylene (**19**)

Yield 86% (colorless crystals obtained by crystallization from diethyl ether); ¹H NMR (200 MHz, CDCl₃, 25°C): δ =7.49–7.58 (m, 2H, Ar), 7.02–7.40 (m, 6H, Ar), 6.86–6.93 (m, 1H, Ar), 3.81 ppm (s, 3H, OCH₃); ¹³C NMR (50.32 MHz, CDCl₃, 25°C): δ =159.3, 131.6, 129.4, 128.3, 128.2, 124.2, 124.1, 123.2, 116.3, 114.9, 89.3, 89.2, 55.2 ppm; IR (KBr): $\tilde{\nu}$ =3049 (w), 3005 (w), 2950 (w), 2829 (w), 1598 (s), 1580 (s), 1492 (s), 1464 (s), 1440 (m), 1418 (m), 1321 (m), 1234 (s), 1036 (w), 924 (w), 862 (m), 793 (s), 768 (s), 686 cm⁻¹ (s); MS (70 eV, EI) *m/z* (%)=208 (100, *M*⁺), 178 (29), 165 (17); *R*_f=0.69 (*n*-hexane/ethyl acetate 4.5:1).

(2-Fluorophenyl)phenylacetylene (**21**)

Yield 73%; ¹H NMR (200 MHz, CDCl₃, 25°C): δ =7.01–7.62 ppm (m, Ar); ¹³C NMR (50.32 MHz, CDCl₃, 25°C): δ =165.1, 160.1, 133.41, 133.39, 131.7, 130.0, 129.8, 128.5, 128.3, 123.94, 123.87, 122.9, 115.7, 115.3, 112.1, 111.7, 94.43, 94.36, 82.6 ppm; ¹⁹F NMR (188.33 MHz, CDCl₃, 25°C): δ =-106 - -109.8 ppm (m); IR (KBr): $\tilde{\nu}$ =3061 (w), 1595 (m), 1270 (m), 1497 (s), 1443 (s), 1263 (m), 1221 (s), 1098 (m), 1028 (m), 943 (w), 916 (w), 858 (w), 795 (m), 755 (s), 689 (s), 580 cm⁻¹ (w); MS (70 eV, EI) *m/z* (%)=196 (100, *M*⁺), 170 (11), 98 (13); *R*_f=0.66 (*n*-hexane/ethyl acetate 4.5:1).

(3-Methylphenyl)phenylacetylene (**16**)

Yield 89%; ¹H NMR (200 MHz, CDCl₃, 25°C): δ =7.50–7.61 (m, 2H), 7.08–7.44 (m, 10H), 2.37 ppm (s, 3H, CH₃); ¹³C NMR (50.32 MHz, CDCl₃, 25°C): δ =138.0, 132.2, 131.6, 123.4, 123.1, 129.1, 128.7, 128.3, 128.2, 128.1, 89.6, 89.0, 21.2 ppm; IR (KBr): $\tilde{\nu}$ =3056 (w), 2912 (w), 1601 (m), 1493 (s), 1442 (m), 1070 (w), 913 (w), 783 (s), 755 (s), 689 (s), 544 cm⁻¹ (w); MS (70 eV, EI) *m/z* (%)=192 (100, *M*⁺), 165 (18), 95 (15), 82 (12); *R*_f=0.66 (*n*-hexane/ethyl acetate 4.5:1).

(4-tert-Butylphenyl)phenylacetylene (**17**)

Yield 73%; ¹H NMR (200 MHz, CDCl₃, 25°C): δ =6.730–7.69 (m, 9H, Ar), 1.44 ppm (s, 9H, C(CH₃)₃); ¹³C NMR (50.32 MHz, CDCl₃, 25°C): δ =151.4, 131.5, 131.3, 128.2, 128.0, 125.3, 123.5, 120.2, 89.5, 88.7, 34.7, 31.1 ppm; IR (KBr): $\tilde{\nu}$ =2963 (s), 1595 (m), 1504 (m), 1442 (m), 1396 (w), 1363 (m), 1268 (w), 1103 (w), 1069 (w), 913 (w), 836 (s), 754 (s), 690 (s), 562 cm⁻¹ (m); MS (70 eV, EI) *m/z* (%)=234 (68, *M*⁺), 219 (100), 203 (17), 191 (19), 178 (12), 96 (27); *R*_f=0.53 (*n*-hexane/ethyl acetate 4.5:1).

Phenyl(2-pyridinyl)acetylene (**23**)

Yield 88% (colorless crystals obtained by crystallization from diethyl ether); ¹H NMR (200 MHz, CDCl₃, 25°C): δ =8.46–8.52 (m, 1H, Ar), 7.35–7.57 (m, 4H, Ar), 7.18–7.28 (m, 3H, Ar), 7.04–7.13 ppm (m, 1H, Ar); ¹³C NMR (50.32 MHz, CDCl₃, 25°C): δ =149.8, 143.2, 135.9, 131.8, 128.8, 128.2, 126.9, 122.9, 122.0, 88.5, 89.0 ppm; IR (KBr): $\tilde{\nu}$ =3049 (w), 2214 (m), 1595 (w), 1579 (s), 1561 (m), 1491 (s), 1441 (m), 1426 (s), 1153 (m), 777 (m), 756 (m), 688 cm⁻¹ (m); MS (70 eV, EI) *m/z* (%)=179 (100, *M*⁺), 151 (16), 76 (17); *R*_f=0.29 (*n*-hexane/ethyl acetate 4.5:1).

General Procedure for the Reduction of Alkynes

A pressure tube was charged with diiron nonacarbonyl (0.036 mmol, 5.0 mol %). The catalyst was dissolved in freshly distilled tetrahydrofuran (2.0 mL). To this solution diphenylacetylene (0.72 mmol), (EtO)₃SiH (0.79 mmol) were added via syringe. The reaction mixture was stirred in a preheated oil bath at 60°C for 24 h. The mixture was cooled down in an ice bath and was treated with dodecane (10 μ L) as GC standard (for GC-analysis), and aqueous sodium hydroxide solution (1.0 mL) with stirring. The reaction mixture was stirred for 60 min at RT and was then extracted with diethyl ether (2 \times 10.0 mL). The combined organic layers were washed with brine, dried over anhydrous Na₂SO₄, filtered (an aliquot was removed for GC-analysis), and concentrated in vacuum. The yield was monitored by GC (30 m Rx-5 ms column, 40–300°C) and by ¹H NMR spectroscopy. The crude product was purified over a short plug of silica gel (eluent: ethyl acetate). The analytical data for all products are in agreement with literature reports.^[20]

1-(4-Methylphenyl)-2-phenyl ethene (**15a**)

¹H NMR (200 MHz, CDCl₃, 25°C): δ =Selected data for the (*Z*) isomer: 6.52 (s, 2H, C(H)=C(H)), 2.27 (s, 3H, CH₃), Selected data for the (*E*) isomer: 2.35 (s, 3H, CH₃) ppm; MS (70 eV, EI) *m/z* (%) for the (*Z*) isomer: 194 (87, *M*⁺), 179 (100), 165 (11), 152 (11), 115 (13), 96 (14); (*E*) isomer: 194 (84, *M*⁺), 188 (10), 179 (100), 165 (11), 152 (11), 115 (14), 105 (12), 92 (12), 89 (15), 76 (12); GC (30 m Rx-5 ms column, 40–300°C) for the (*Z*)-isomer 8.492 min, (*E*)-isomer 9.725 min.

1-(3-Methylphenyl)-2-phenyl ethene (**16a**)

¹H NMR (200 MHz, CDCl₃, 25°C): δ =Selected data for the (*Z*)-isomer: 6.53 (s, 2H, C(H)=C(H)), 2.28 (s, 3H, CH₃), Selected data for the (*E*)-isomer: 2.36 (s, 3H, CH₃) ppm; MS (70 eV, EI) *m/z* (%) for (*Z*) isomer: 194 (89, *M*⁺), 179 (100), 165 (10), 115 (12), 96 (11), 89 (11); (*E*) isomer: 194 (92, *M*⁺), 179 (100), 165 (11), 115 (15), 96 (18), 89 (15); GC (30 m Rx-5 ms column, 40–300°C): (*Z*)-isomer 8.650 min, (*E*)-isomer 9.783 min.

1-(4-tert-Butylphenyl)-2-phenyl ethene (**17a**)

Selected data for the (*Z*)-isomer: 1.49 (s, 9H, CH₃), Selected data for the (*E*)-isomer: 1.37 (s, 9H, CH₃) ppm; MS (70 eV, EI) *m/z* (%) for isomer 1: 236 (50, *M*⁺), 221 (100), 178 (12), 91 (26); isomer 2: 236 (49, *M*⁺), 221

(100), 178 (11), 96 (11), 91 (22). Isomer 1: 9.808 min, isomer 2: 11.025 min.

1-(4-Methoxyphenyl)-2-phenyl ethene (18a)

¹H NMR (200 MHz, CDCl₃, 25 °C): δ=Selected data for the (Z)-isomer: 3.75 (s, 3H, CH₃), Selected data for the (E)-isomer: 3.79 (s, 3H, CH₃) ppm; MS (70 eV, EI) *m/z* (%) for isomer 1: 210 (100, M⁺), 195 (24), 179 (18), 165 (33), 152 (25), 89 (12); isomer 2: 210 (100, M⁺), 195 (18), 179 (129), 165 (22), 152 (14). Isomer 1: 9.575 min, isomer 2: 10.633 min.

1-(3-Methoxyphenyl)-2-phenyl ethene (19a)

¹H NMR (200 MHz, CDCl₃, 25 °C): δ=Selected data for the (Z)-isomer: 3.63 (s, 3H, CH₃), Selected data for the (E)-isomer: 3.75 (s, 3H, CH₃) ppm; MS (70 eV, EI) *m/z* (%) for isomer 1: 210 (100, M⁺), 194 (26), 179 (39), 167 (18), 152 (17), 89 (10); isomer 2: 210 (100, M⁺), 194 (22), 179 (32), 165 (26), 152 (13), 105 (21). Isomer 1: 9.350 min, isomer 2: 10.508 min.

1-(4-Fluorophenyl)-2-phenyl ethene (20a)

¹³C NMR (50 MHz, CDCl₃, 25 °C): δ=Selected data for the (Z)-isomer: 163.4, Selected data for the (E)-isomer: 162.4 ppm; MS (70 eV, EI) *m/z* (%) for isomer 1: 198 (100, M⁺), 183 (37), 176 (30), 98 (11); isomer 2: 198 (100, M⁺), 183 (37), 177 (29), 98 (29), 85 (12). Isomer 1: 7.967 min, isomer 2: 9.100 min.

1-(2-Fluorophenyl)-2-phenyl ethene (21a)

¹³C NMR (50 MHz, CDCl₃, 25 °C): δ=Selected data for the (Z)-isomer: 162.2, Selected data for the (E)-isomer: 158.3 ppm; MS (70 eV, EI) *m/z* (%) for isomer 1: 198 (100, M⁺), 183 (35), 177 (30), 98 (14); 198 (100, M⁺), 183 (34), 177 (22), 120 (10), 98 (27), 89 (12), 85 (17). Isomer 1: 7.967 min, isomer 2: 9.075 min.

1-(4-Nitrophenyl)-2-phenyl ethene (22a)

¹H NMR (200 MHz, CDCl₃, 25 °C): δ=Selected data for the (Z)-isomer: 8.04 (m, 2H), Selected data for the (E)-isomer: 8.20 (m, 2H) ppm; MS (70 eV, EI) *m/z* (%)=(Z)-isomer: 225 (100, M⁺), 178 (73), 152 (18); isomer 2: 225 (86, M⁺), 178 (100), 152 (30), 89 (19), 76 (20); (Z)-isomer: 10.650 min, isomer 2: 11.733 min.

1-Phenyl-2-(2-pyridinyl) ethylene (23a)

¹³C NMR (50 MHz, CDCl₃, 25 °C): δ=Selected data for the (Z)-isomer: 156.2, Selected data for the (E)-isomer: 155.8 ppm; MS (70 eV, EI) *m/z* (%) for isomer 1: 180 (100, M⁺), 152 (10); isomer 2: 180 (100, M⁺), 152 (10); isomer 1: 8.425 min, isomer 2: 9.408 min.

1-Phenyl-1-hexene (24a)

¹H NMR (200 MHz, CDCl₃, 25 °C): δ=Selected data for the (Z)-isomer: 5.67 (m, 1H) ppm; MS (70 eV, EI) *m/z* (%) for the (Z)-isomer: 160 (27, M⁺), 117 (100), 104 (79), 91 (32); GC (30 m Rxi-5 ms column, 40–300 °C): (Z)-isomer: 6.242 min.

Styrene (25a)

MS (70 eV, EI) *m/z* (%)=150 (100, M⁺), 135 (94), 117 (72), 109 (58), 91 (26), 77 (16), 72 (11), 69 (19), 65 (45), 51 (22); GC (30 m Rxi-5 ms column, 40–300 °C): 5.892 min.

1,4-Diphenyl-1-butene-3-yne (26a)

¹H NMR (200 MHz, CDCl₃, 25 °C): δ=Selected data for the (Z)-isomer: 5.92 (d, 1H, *J*=12.0 Hz, C(H)=C(H)), Selected data for the (E)-isomer: 6.40 (d, 1H, *J*=16.1 Hz, C(H)=C(H)) ppm; MS (70 eV, EI) *m/z* (%) for the (Z)-isomer: 204 (100, M⁺), 101 (31), 89 (12), 76 (12); (E)-isomer: 204 (100, M⁺), 101 (38), 89 (17), 76 (18); GC (30 m Rxi-5 ms column, 40–300 °C): (Z)-isomer 10.117 min, (E)-isomer 10.667 min.

Phenyl allyl thioether (27a)

¹³C NMR (50 MHz, CDCl₃, 25 °C): δ=37.5 (SCH₂), 118.0 (C=C) ppm; MS (70 eV, EI) *m/z* (%): 150 (100, M⁺), 135 (94), 117 (72), 109 (58), 91

(26), 77 (16), 72 (11), 69 (19), 65 (45), 51 (22); GC (30 m Rxi-5 ms column, 40–300 °C): 5.892 min.

Ethyl cinnamate (28a)

¹H NMR (200 MHz, CDCl₃, 25 °C): δ=Selected data for the (Z)-isomer: 6.95 (d, 2H, C(H)=C(H)), 2.27 (s, 3H, CH₃), Selected data for the (E)-isomer: 6.41 (d, 2H, C(H)=C(H)), 7.66 (d, 2H) ppm; MS (70 eV, EI) *m/z* (%) for the (Z)-isomer: 176 (25, M⁺), 148 (14), 131 (100), 103 (60), 77 (39), 51 (18); (E)-isomer: 176 (26, M⁺), 148 (14), 131 (100), 103 (56), 77 (36), 51 (17); GC (30 m Rxi-5 ms column, 40–300 °C): (Z)-isomer 7.042 min, (E)-isomer 7.633 min.

2-Butenedioic acid dimethyl ester (29a)

¹H NMR (200 MHz, CDCl₃, 25 °C): δ=Selected data for the (Z)-isomer: 6.22 (s, 2H, -C(H)=C(H)-), 3.76 (s, 3H, OCH₃), Selected data for the (E)-isomer: 6.87 (s, 2H, -C(H)=C(H)-), 3.81 (s, 3H, OCH₃) ppm; MS (70 eV, EI) *m/z* (%) for the (Z)-isomer: 144 (2, M⁺), 113 (100), 59 (55); (E)-isomer: 143 (1, M⁺), 126 (28), 113 (100), 99 (70), 85 (38) 82 (27), 59 (35), 55 (35); GC (30 m Rxi-5 ms column, 40–300 °C): (Z)-isomer 4.283 min, (E)-isomer 4.925 min.

2-Butenedioic acid diethyl ester (30a)

¹H NMR (200 MHz, CDCl₃, 25 °C): δ=Selected data for the (Z)-isomer: 6.26 (s, 2H, C(H)=C(H)), Selected data for the (E)-isomer: 6.83 (d, 2H, C(H)=C(H)) ppm; MS (70 eV, EI) *m/z* (%) for the (Z)-isomer: 172 (1, M⁺), 127 (30), 99 (100); (E)-isomer: 172 (1, M⁺), 127 (100), 99 (77), 82 (16), 71 (15), 55 (31); GC (30 m Rxi-5 ms column, 40–300 °C): (Z)-isomer 5.442 min, (E)-isomer 5.550 min.

Bis-(trimethylsilyl)ethylene (31a)

¹H NMR (200 MHz, CDCl₃, 25 °C): δ=Selected data for the (Z)-isomer: 0.13 (s, 18H, Si(CH₃)₃), Selected data for the (E)-isomer: 0.06 (s, 18H, Si(CH₃)₃) ppm; MS (70 eV, EI) *m/z* (%) for the (Z)-isomer: 172 (2, M⁺), 125 (12), 99 (12), 73 (100), 59 (15); (E)-isomer: 172 (5, M⁺), 157 (13), 99 (13), 73 (100); GC (30 m Rxi-5 ms column, 40–300 °C): (Z)-isomer 3.042 min, (E)-isomer 3.533 min.

General Synthesis of Iron Phosphane Complexes

A solution of the corresponding phosphine ligand (761 μmol) and diiron nonacarbonyl (761 μmol) in diethyl ether (30 mL) was refluxed for 1–2 h. The solution was allowed to cool to room temperature. The volatiles were removed under vacuum to yield a brown foam. The products were purified by extraction and filtration through a pad of aluminum oxide. Colored crystals were obtained by crystallization from diethyl ether.

Compound 41

Reaction time: 1 h, deep-red crystals obtained from diethyl ether; ¹H NMR (200 MHz, C₆D₆, 25 °C): δ=7.98–7.82 (m, Ar), 7.10–6.94 (m, Ar), 4.29 (s, 4H, Cp), 3.83 ppm (s, 4H, Cp); IR (KBr): ν=3056 (w), 1981 (s), 1907 (s), 1879 (s), 1480 (m), 1434 (m), 1309 (w), 1162 (w), 1089 (m), 1038 (w), 821 (w), 750 (w), 697 (m), 634 (m), 610 (w), 544 (w), 499 (w), 467 cm⁻¹ (w); MS (70 eV, EI) *m/z* (%)=694 (M⁺), 638 (10), 610 (100), 554 (27), 425 (35), 304 (18).

Compound 42

Reaction time: 2 h, deep-red crystals obtained from diethyl ether; ¹H NMR (200 MHz, C₆D₆, 25 °C): δ=7.15–6.88 (m, Ar), 6.46–6.05 (m, Ar), 3.22 ppm (brs, 18H, OM₂); IR (KBr): ν=3001 (w), 2970 (w), 2940 (m), 2839 (m), 2536 (w), 2028 (s), 1912 (s), 1580 (s), 1468 (s), 1427 (s), 1251 (s), 1182 (w), 1171 (w), 1149 (w), 1105 (s), 1029 (m), 899 (w), 776 (s), 757 (m), 719 (m), 627 (s), 604 (w), 531 (m), 484 cm⁻¹ (m); MS (70 eV, EI) *m/z* (%)=526 (46), 498 (62), 442 (62), 411 (36), 396 (27), 365 (12), 291 (25), 249 (14), 167 (14), 151 (100), 138 (28), 91 (18), molecular ion peak was not detectable.

Single-Crystal X-ray Structure Determination

Single-crystals were mounted on a glass capillary in perfluorinated oil and measured under a flow of cold N₂. The data were collected on an Oxford Diffraction Xcalibur S Sapphire spectrometer at 150(2) K (Mo_{Kα} radiation, $\lambda=0.71073\text{ \AA}$). The structures were solved by direct methods and refined on F² with the SHEXL-97 software package.^[22] The positions of the hydrogen atoms were calculated and considered isotropically according to a riding model.

CCDC 804100 (**41**) and CCDC 804101 (**42**) contain the supplementary crystallographic data for this paper. These data can be obtained free of charge from the Cambridge Crystallographic Data Centre via www.ccdc.cam.ac.uk/data_request/cif.

Compound **41**

Monoclinic; space group $P2_1/n$; $a=10.7997(3)$, $b=23.8533(6)$, $c=11.1565(3)\text{ \AA}$; $\alpha=90^\circ$, $\beta=105.316(3)^\circ$, $\gamma=90^\circ$; $V=2771.94(14)\text{ \AA}^3$; $Z=4$; $\rho_{\text{calc}}=1.462\text{ mg m}^{-3}$; Absorption coefficient 0.659 mm⁻¹; F(000) 1264; Reflections collected: 20394; Independent reflections: 4872 [$R_{\text{int}}=0.0402$]; Completeness to $\theta=25.00^\circ$ (99.7%); Max. and min. transmission 0.8741 and 0.8422; Goodness-of-fit on F² 0.963; Final R indices [$I>2\sigma(I)$]: $R_1=0.0346$, $wR_2=0.0730$; R indices (all data): $R_1=0.0532$, $wR_2=0.0772$; Largest diff. peak and hole 0.381 and -0.279 e \AA^{-3} .

Compound **42**

Monoclinic; space group $P2_1/c$; $a=9.6588(3)$, $b=16.1075(5)$, $c=19.7701(7)\text{ \AA}$; $\alpha=90^\circ$, $\beta=95.443(4)^\circ$, $\gamma=90^\circ$; $V=3061.95(17)\text{ \AA}^3$; $Z=4$; $\rho_{\text{calc}}=1.488\text{ mg m}^{-3}$; Absorption coefficient 1.089 mm⁻¹; F(000) 1392; Reflections collected: 12340; Independent reflections: 5379 [$R_{\text{int}}=0.0279$]; Completeness to $\theta=25.00^\circ$ (99.7%); Max. and min. transmission: 0.7956 and 0.6824; Goodness-of-fit on F² 1.001; Final R indices [$I>2\sigma(I)$]: $R_1=0.0368$, $wR_2=0.0951$; R indices (all data): $R_1=0.0514$, $wR_2=0.0992$; Largest diff. peak and hole 0.715 and -0.358 e \AA^{-3} .

Acknowledgements

This work was supported by the Cluster of Excellence “Unifying Concepts in Catalysis” (sponsored by the Deutsche Forschungsgemeinschaft and administered by the Technische Universität Berlin). The authors thank M. Weidner (TU Berlin) for technical support. Dr. K. Junge (Leibniz Institut für Katalyse e.V. an der Universität Rostock) is acknowledged for the kind donation of ligand **11**.

- [1] *The Handbook of Homogeneous Hydrogenation* (Eds.: J. G. de Vries, C. J. Elsevier), **2006**, Wiley-VCH, Weinheim.
- [2] For leading reference see: palladium-catalyzed: a) V. Jurčík, S. P. Nolan, C. S. L. Cazin, *Chem. Eur. J.* **2009**, *15*, 2509–2511; b) J. W. Sprengers, J. Wassenaar, N. D. Clement, K. J. Cavell, C. J. Elsevier, *Angew. Chem.* **2005**, *117*, 2062–2065; *Angew. Chem. Int. Ed.* **2005**, *44*, 2026–2029; c) A. M. Kluwer, T. S. Koblenz, T. Jonischkeit, K. Woelk, C. J. Elsevier, *J. Am. Chem. Soc.* **2005**, *127*, 15470–15480; d) M. W. van Laren, M. A. Duin, C. Clerk, M. Naglia, D. Rogolino, P. Pelagatti, A. Bacchi, C. Pelizzi, C. J. Elsevier, *Organometallics* **2002**, *21*, 1546–1553; e) M. Costa, P. Pelagatti, C. Pelizzi, D. Rogolino, *J. Mol. Catal. A* **2002**, *178*, 21–26; f) M. W. van Laren, C. J. Elsevier, *Angew. Chem.* **1999**, *111*, 3926–3929; *Angew. Chem. Int. Ed.* **1999**, *38*, 3715–137; g) P. Pelagatti, A. Venturini, A. Leporati, M. Carelli, M. Costa, A. Bacchi, G. Pelizzi, C. Pelizzi, *J. Chem. Soc. Dalton Trans.* **1998**, 2715–2721; h) B. M. Trost, R. Braslau, *Tetrahedron Lett.* **1989**, *30*, 4657–4660; ruthenium-catalyzed: i) C. Belger, N. M. Neisius, B. Plietker, *Chem. Eur. J.* **2010**, *16*, 12214–12220; j) H. H. Horváth, F. Joó, *React. Kinet. Catal. Lett.* **2005**, *85*, 355–360; k) Y. Gao, M. C. Jennings, R. J. Puddephatt, *Can. J. Chem.* **2001**, *79*, 915–921; l) Y. Shvo, I. Goldberg, D. Czerkie, D. Reshef, Z. Stein, *Organometallics* **1997**, *16*, 133–138; rhodium-catalyzed: m) N.

Kameda, T. Yoneda, *J. Chem. Soc. Jpn.* **1999**, *1*, 33–36; n) R. R. Schrock, J. A. Osborn, *J. Am. Chem. Soc.* **1976**, *98*, 2143–2147.

- [3] a) R. H. Morris, *Chem. Soc. Rev.* **2009**, *38*, 2282–2291; b) S. Enthalter, K. Junge, M. Beller, *Angew. Chem.* **2008**, *120*, 3363–3367; *Angew. Chem. Int. Ed.* **2008**, *47*, 3317–3321; c) *Iron Catalysis in Organic Chemistry* (Ed.: B. Plietker), Wiley-VCH, Weinheim, **2008**; d) S. Gaillard, J.-L. Renaud, *ChemSusChem* **2008**, *1*, 505–509; e) A. Correa, O. G. Mancheño, C. Bolm, *Chem. Soc. Rev.* **2008**, *37*, 1108–1117; f) B. D. Sherry, A. Fürstner, *Acc. Chem. Res.* **2008**, *41*, 1500–1511; g) R. M. Bullock, *Angew. Chem.* **2007**, *119*, 7504–7507; *Angew. Chem. Int. Ed.* **2007**, *46*, 7360–7363; h) C. Bolm, J. Legros, J. Le Pailh, L. Zani, *Chem. Rev.* **2004**, *104*, 6217–6254.
- [4] See leading references and citation within: a) Y. Sunada, H. Kawakami, T. Imaoka, Y. Motoyama, H. Nagashima, *Angew. Chem.* **2009**, *121*, 9675–9678; *Angew. Chem. Int. Ed.* **2009**, *48*, 9511–9514; b) S. Zhou, K. Junge, D. Addis, S. Das, M. Beller, *Angew. Chem.* **2009**, *121*, 9671–9674; *Angew. Chem. Int. Ed.* **2009**, *48*, 9507–9510; c) S. Zhou, S. Fleischer, K. Junge, S. Das, D. Addis, M. Beller, *Angew. Chem.* **2010**, *122*, 8298–8302; *Angew. Chem. Int. Ed.* **2010**, *49*, 8121–8125; d) A. M. Tondreau, J. M. Darmon, B. M. Wile, S. K. Floyd, E. Lobkovsky, P. J. Chirik, *Organometallics* **2009**, *28*, 3928–3940; e) N. Meyer, A. J. Lough, R. H. Morris, *Chem. Eur. J.* **2009**, *15*, 5605–5610; f) A. Mikhailine, A. J. Lough, R. H. Morris, *J. Am. Chem. Soc.* **2009**, *131*, 1394–1395; g) C. Sui-Seng, F. N. Haque, A. Hadzovic, A.-M. Pütz, V. Reuss, N. Meyer, A. J. Lough, M. Z.-D. Luliis, R. H. Morris, *Inorg. Chem.* **2009**, *48*, 735–743.
- [5] a) C. Rangheard, C. de Julián Fernández, P.-H. Phua, J. Hoorn, L. Lefort, J. G. De Vries, *Dalton Trans.* **2010**, *39*, 8464–8471; b) P.-H. Phua, L. Lefort, J. A. F. Boogers, M. Tristany, J. G. de Vries, *Chem. Commun.* **2009**, 3747–3749; c) R. J. Trovitch, E. Lobkovsky, E. Bill, P. J. Chirik, *Organometallics* **2008**, *27*, 1470–1478; d) E. J. Daida, J. C. Peters, *Inorg. Chem.* **2004**, *43*, 7474–7485; e) M. Takeuchi, K. Kano, *Organometallics* **1993**, *12*, 2059–2064; f) C. Bianchini, A. Meli, M. Peruzzini, P. Frediani, C. Bohanna, M. A. Esteruelas, L. A. Oro, *Organometallics* **1992**, *11*, 138–145; g) Y. Nitta, Y. Hiramatsu, Y. Okamoto, T. Imanaka, *Stud. Surf. Sci. Catal.* **1991**, *63*, 103–112; h) C. U. Pittman Jr., R. C. Ryan, J. McGee, *J. Organomet. Chem.* **1979**, *178*, C43–C49; i) J. J. Brunet, P. Caubere, *Tetrahedron Lett.* **1977**, *18*, 3947–3950.
- [6] a) K. R. Campos, D. Cai, M. Journet, J. J. Kowal, R. D. Larsen, R. J. Reider, *J. Org. Chem.* **2001**, *66*, 3634–3635; b) M. Gruttaduria, R. Noto, G. Deganello, L. F. Liotta, *Tetrahedron Lett.* **1999**, *40*, 2857–2857; c) N. M. Yoon, K. B. Park, H. J. Lee, J. Choi, *Tetrahedron Lett.* **1996**, *37*, 8527–8528; d) J. Choi, N. M. Yoon, *Tetrahedron Lett.* **1996**, *37*, 1057–1060; e) B. M. Choudary, G. V. M. Sharma, P. Bharath, *Angew. Chem.* **1989**, *101*, 506–507; *Angew. Chem. Int. Ed. Engl.* **1989**, *28*, 465–466; *Angew. Chem. Int. Ed. Engl.* **1989**, *28*, 465–466; f) J.-J. Brunet, P. Caubere, *J. Org. Chem.* **1984**, *49*, 4058–4060; g) D. Savoia, E. Tagliavini, C. Trombini, A. Umani-Ronchi, *J. Org. Chem.* **1981**, *46*, 5340–5343; h) P. Gallois, J.-J. Brunet, P. Caubere, *J. Org. Chem.* **1980**, *45*, 1946–1950; i) N. A. Cortese, R. F. Heck, *J. Org. Chem.* **1978**, *43*, 3985–3987.
- [7] *Metal-catalyzed cross-coupling reactions* (Eds.: F. Diederich, P. J. Stang.) Wiley-VCH, Weinheim, **1999**.
- [8] S. C. Bart, E. Lobkovsky, P. J. Chirik, *J. Am. Chem. Soc.* **2004**, *126*, 13794–13807.
- [9] S. Enthalter, *ChemCatChem* **2011**, *4*, 666–670.
- [10] a) S. Enthalter, K. Schröder, S. Inoue, B. Eckhardt, K. Junge, M. Beller, M. Driess, *Eur. J. Org. Chem.* **2010**, 4893–4901; b) K. Schröder, S. Enthalter, B. Join, K. Junge, M. Beller, *Adv. Synth. Catal.* **2010**, *352*, 1771–1778; c) S. Enthalter, *ChemCatChem* **2010**, *2*, 1411–1415.
- [11] a) A. Suárez, M. A. Méndez-Rojas, A. Pizzano, *Organometallics* **2002**, *21*, 4611–4621; b) S. M. Socol, J. G. Verkade, *Inorg. Chem.* **1984**, *23*, 3487–3491; c) D. W. Allen, B. F. Taylor, *J. Chem. Soc. Dalton Trans.* **1982**, 51–54.
- [12] See for the phosphorous selen coupling constants: a) H. Liu, J. S. Owen, A. P. Alivisatos, *J. Am. Chem. Soc.* **2007**, *129*, 305–312; b) D. W. Allen, I. W. Nowell, B. F. Taylor, *J. Chem. Soc. Dalton*

- Trans.* **1985**, 2505–2508; c) A. G. Sergeev, A. Spannenberg, M. Beller, *J. Am. Chem. Soc.* **2008**, 130, 15549–15563; d) M. N. Chevkalova, L. F. Manzhukova, N. V. Artemova, Yu. N. Luzikov, I. E. Nifantév, E. E. Nifantév, *Russ. Chem. Bull. Int. Ed.* **2003**, 52, 78–84; e) P. A. W. Dean, *Can. J. Chem.* **1979**, 57, 754–761.
- [13] C. Hansch, A. Leo, R. W. Taft, *Chem. Rev.* **1991**, 91, 165–195.
- [14] Gaussian 03, Revision E.01, M. J. Frisch, G. W. Trucks, H. B. Schlegel, G. E. Scuseria, M. A. Robb, J. R. Cheeseman, J. A. Montgomery, Jr., T. Vreven, K. N. Kudin, J. C. Burant, J. M. Millam, S. S. Iyengar, J. Tomasi, V. Barone, B. Mennucci, M. Cossi, G. Scalmani, N. Rega, G. A. Petersson, H. Nakatsuji, M. Hada, M. Ehara, K. Toyota, R. Fukuda, J. Hasegawa, M. Ishida, T. Nakajima, Y. Honda, O. Kitao, H. Nakai, M. Klene, X. Li, J. E. Knox, H. P. Hratchian, J. B. Cross, V. Bakken, C. Adamo, J. Jaramillo, R. Gomperts, R. E. Stratmann, O. Yazyev, A. J. Austin, R. Cammi, C. Pomelli, J. W. Ochterski, P. Y. Ayala, K. Morokuma, G. A. Voth, P. Salvador, J. J. Dannenberg, V. G. Zakrzewski, S. Dapprich, A. D. Daniels, M. C. Strain, O. Farkas, D. K. Malick, A. D. Rabuck, K. Raghavachari, J. B. Foresman, J. V. Ortiz, Q. Cui, A. G. Baboul, S. Clifford, J. Cioslowski, B. B. Stefanov, G. Liu, A. Liashenko, P. Piskorz, I. Komaromi, R. L. Martin, D. J. Fox, T. Keith, M. A. Al-Laham, C. Y. Peng, A. Nanayakkara, M. Challacombe, P. M. W. Gill, B. Johnson, W. Chen, M. W. Wong, C. Gonzalez, J. A. Pople, Gaussian, Inc., Wallingford CT, **2004**.
- [15] a) K. Wolinski, J. F. Hilton, P. Pulay, *J. Am. Chem. Soc.* **1990**, 112, 8251–8260; b) R. Ditchfield, *Mol. Phys.* **1974**, 27, 789–807; c) R. McWeeny, *Phys. Rev.* **1962**, 126, 1028–1034.
- [16] M. Rubin, A. Trofimov, V. Gevorgyan, *J. Am. Chem. Soc.* **2005**, 127, 10243–10249.
- [17] a) J. A. S. Howell, N. Fey, J. D. Lovatt, P. C. Yates, P. McArdle, D. Cunningham, E. Sadeh, H. E. Gottlieb, Z. Goldschmidt, M. B. Hursthouse, M. E. Light, *Dalton Trans.* **1999**, 3015–3028; b) M. Haberberger, E. Irran, S. Enthalier, *Eur. J. Inorg. Chem.* **2011**, DOI: 10.1002/ejic.201100233.
- [18] T.-J. Kim, K.-H. Kwon, S.-C. Kwon, J.-O. Baeg, S.-C. Shim, *J. Organomet. Chem.* **1990**, 389, 205–217.
- [19] a) J. T. Guan, G.-A. Yu, L. Chen, W. T. Qing, J. J. Yuan, S. H. Liu, *Appl. Organomet. Chem.* **2009**, 23, 75–77; b) S. B. Park, H. Alper, *Chem. Commun.* **2004**, 1306–1307; c) N. Sakai, K. Annaka, T. Konakahara, Takeo, *Org. Lett.* **2004**, 6, 1527–1530; d) J. H. Li, J. L. Li, D. P. Wang, S. F. Pi, Y. X. Xie, M. B. Zhang, X. C. Hu, *J. Org. Chem.* **2007**, 72, 2053–2057; e) M. Bandini, R. Luque, V. Budarin, D. J. Macquarrie, *Tetrahedron* **2005**, 61, 9860–9868; f) G. Hennrich, M. T. Murillo, P. Prados, H. Al-Saraierh, A. El-Dali, D. W. Thompson, J. Collins, P. E. Georgiou, A. Teshome, I. Asselberghs, Inge; K. Clays, *Chem. Eur. J.* **2007**, 13, 7753–7761; K. Clays, *Chem. Eur. J.* **2007**, 13, 7753–7761; g) R. Cellia, H. A. Stefani, *Tetrahedron* **2006**, 62, 5656–5662; h) F. Alonso, P. Riente, M. Yus, *Eur. J. Org. Chem.* **2009**, 6034–6042.
- [20] a) S. Yasuda, H. Yorimitsu, K. Oshima, *Organometallics* **2010**, 29, 2634–2636; b) F. Luo, C. Pan, W. Wang, Z. Ye, J. Cheng, *Tetrahedron* **2010**, 66, 1399–1403; c) F. Li, T. S. A. Hor, *Adv. Synth. Catal.* **2008**, 350, 2391–2400; d) J. C. Roberts, J. A. Pincock, *J. Org. Chem.* **2004**, 69, 4279–4282; e) H. Zhao, Y. Wang, J. Sha, S. Sheng, M. Cai, *Tetrahedron* **2008**, 64, 7517–7523; f) J. McNulty, P. Das, *Eur. J. Org. Chem.* **2009**, 4031–4035; g) J. Li, R. Hua, T. Liu, *J. Org. Chem.* **2010**, 75, 2966–2970; h) C. Walter, M. Oestreich, *Angew. Chem.* **2008**, 120, 3878–3880; *Angew. Chem. Int. Ed.* **2008**, 47, 3818–3820; i) M. Mahesh, J. A. Murphy, H. P. Wessel, *J. Org. Chem.* **2005**, 70, 4118–4123; j) K. Karabelas, A. Hallberg, *J. Org. Chem.* **1986**, 51, 5286–5290; k) B. Marciniec, C. Pietraszuk, Z. Foltynowicz, *J. Organomet. Chem.* **1994**, 474, 83–87; l) T. Yoshino, S. Imori, H. Togo, Hideo, *Tetrahedron* **2006**, 62, 1309–1317; m) M. Nishiura, Z. Hou, Y. Wakatsuki, T. Yamaki, T. Miyamoto, *J. Am. Chem. Soc.* **2003**, 125, 1184–1185.
- [21] S. C. Berk, S. L. Buchwald, *J. Org. Chem.* **1992**, 57, 3751–3753.
- [22] G. M. Sheldrick, SHELXL93, Program for the Refinement of Crystal Structures, University of Göttingen, Göttingen, Germany, **1997**.

Received: December 29, 2010

Published online: May 19, 2011